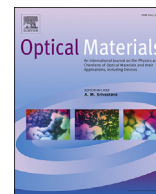




Contents lists available at ScienceDirect

Optical Materials

journal homepage: www.elsevier.com/locate/optmat

Luminescence properties of Eu^{3+} -doped Lanthanum gadolinium hafnates transparent ceramics

Zhengjuan Wang, Guohong Zhou^{*}, Jian Zhang, Xianpeng Qin, Shiwei Wang^{*}

State Key Laboratory of High Performance Ceramics and Superfine Microstructure, Shanghai Institute of Ceramics, Chinese Academy of Sciences, Shanghai 200050, China

ARTICLE INFO

Article history:

Received 13 March 2016

Received in revised form

13 May 2016

Accepted 25 May 2016

Available online xxx

Keywords:

 Eu^{3+} -doped $\text{La}_{0.8}\text{Gd}_{1.2}\text{Hf}_2\text{O}_7$

Transparent ceramics

Vacuum sintering

Annealing process

Luminescence behavior

ABSTRACT

Eu^{3+} -doped Lanthanum gadolinium hafnates ($\text{La}_{0.8}\text{Gd}_{1.2}\text{Hf}_2\text{O}_7$) transparent ceramics with different Eu^{3+} concentration were fabricated by vacuum sintering. XRD results showed all the ceramics are cubic pyrochlore structure. The effects of annealing process on in-line transmittance and luminescence behavior of the Eu^{3+} -doped $\text{La}_{0.8}\text{Gd}_{1.2}\text{Hf}_2\text{O}_7$ transparent ceramics were investigated. Before annealing, the in-line transmittance of the ceramics was low and the luminescence intensity was weak. As Eu^{3+} doping content increased, the transmittance as well as the luminescence intensity decreased. This was ascribed to oxygen vacancy and other defects in the ceramics resulted from the vacuum sintering. After annealing, the transmittance and luminescence intensity were raised, indicating the elimination of oxygen vacancy. Moreover, with the increase of Eu^{3+} doping content from 1 at% to 10 at%, the luminescence intensity increased without concentration quenching.

© 2016 Published by Elsevier B.V.

1. Introduction

In recent years, transparent ceramic scintillators have been developed for applications in radiation detectors, which are widely used for medical diagnostics, industrial inspection, security check, and high energy physics. They will gradually replace the most commonly used single-crystal scintillators, as the fabrication costs can be reduced, the activator concentration can be higher, and uniformity can be enhanced as well.

Since the first commercial used transparent ceramic scintillator ($\text{Y,Gd})_2\text{O}_3\text{:Eu,Pr}$ [1] was introduced by GE in X-CT, a few commercial ceramic scintillators, such as $\text{Gd}_2\text{O}_2\text{S:Pr,Ce,F}$ [2], $\text{Gd}_3\text{Ga}_5\text{O}_{12}\text{:Cr,Ce}$ [3], was subsequently developed. Then, many newly candidates such as $\text{Lu}_2\text{O}_3\text{:Eu}$ [4], YAG:Ce [5,6], YAP:Ce [7], GYAG:Ce [8], LuAG:Ce [9], LuAG:Pr [10], $\text{BaHfO}_3\text{:Ce}$ [11], $\text{SrHfO}_3\text{:Ce}$ [11,12], $\text{La}_2\text{Hf}_2\text{O}_7\text{:Ti}^{4+}$ [13], and $\text{La}_2\text{Hf}_2\text{O}_7\text{:Pr}^{3+}$ [14] were studied.

Lanthanum gadolinium hafnates ($\text{La}_{2-x}\text{Gd}_x\text{Hf}_2\text{O}_7$) transparent ceramics are a new series of materials as scintillator hosts due to their high transparency, high density and effective atomic number. For scintillation application, high density and effective atomic number mean higher X-

ray or γ -ray stopping power. In this work, $\text{La}_{0.8}\text{Gd}_{1.2}\text{Hf}_2\text{O}_7$ was chosen as the host material for its high transparency (76.1%@800 nm) and relatively high density (8.46 g/cm³) [15]. Then, rare earth ions were doped to achieve scintillation luminescence. Ce^{3+} , Ti^{4+} , and Pr^{3+} have already been studied as the activator ions in $\text{RE}_2\text{M}_2\text{O}_7$ ($\text{RE} = \text{Y, La}$; $\text{M} = \text{Ti, Zr, Hf}$) [16] and $\text{La}_2\text{Hf}_2\text{O}_7$ [13,14], but no Ce^{3+} -activated luminescence were found. While, the luminescence property of Eu^{3+} -doped $\text{La}_{2-x}\text{Gd}_x\text{Hf}_2\text{O}_7$ have not been reported. Therefore, Eu^{3+} was chosen as the activator ion in $\text{La}_{0.8}\text{Gd}_{1.2}\text{Hf}_2\text{O}_7$ host and the luminescence behavior was systematically studied. In addition, the luminescence intensity ratio of $^5\text{D}_0\text{--}^7\text{F}_2$ transition and $^5\text{D}_0\text{--}^7\text{F}_1$ transition for Eu^{3+} can be served as an effective probe of the site symmetry where Eu^{3+} was substituted [17]. Therefore, this work can also direct the study on luminescence properties of other rare earth ions doped $\text{La}_{2-x}\text{Gd}_x\text{Hf}_2\text{O}_7$ transparent ceramics.

In this work, combustion method was used to synthesize the precursor powders and Eu^{3+} -doped $\text{La}_{0.8}\text{Gd}_{1.2}\text{Hf}_2\text{O}_7$ transparent ceramics were fabricated by vacuum sintering. The crystal structure, in-line transmittance, and luminescence properties of the Eu^{3+} -doped $\text{La}_{0.8}\text{Gd}_{1.2}\text{Hf}_2\text{O}_7$ transparent ceramics were investigated. The effects of the annealing process on transmittance and luminescence behavior were also studied.

2. Experimental

A simple sol-gel combustion method was used to synthesize the

^{*} Corresponding author.

^{**} Corresponding author.

E-mail addresses: sic_zhough@mail.sic.ac.cn (G. Zhou), swwang51@mail.sic.ac.cn (S. Wang).

Eu^{3+} doped $\text{La}_{0.8}\text{Gd}_{1.2}\text{Hf}_2\text{O}_7$ powders. $\text{La}(\text{NO}_3)_3 \cdot 6\text{H}_2\text{O}$ (99.99%), Gd_2O_3 (99.99%), Eu_2O_3 (99.99%), $\text{Hf}(\text{OH})_4$ (99.99%), and glycine (A.R.) are the starting materials. Firstly, $\text{La}(\text{NO}_3)_3$ solution was prepared by dissolving $\text{La}(\text{NO}_3)_3 \cdot 6\text{H}_2\text{O}$ into deionized water. Gd_2O_3 and Eu_2O_3 were dissolved in excess nitric acid solution respectively to prepare $\text{Gd}(\text{NO}_3)_3$ and $\text{Eu}(\text{NO}_3)_3$ solutions. Similarly, $\text{Hf}(\text{NO}_3)_4$ solution was prepared by dissolving $\text{Hf}(\text{OH})_4$ into excess nitric acid solution. Then, stoichiometric amounts of the nitrates with different Eu^{3+} doping content (1–10 at%) and glycine were mixed respectively, and stirred thoroughly till the solutions were clear. After that an appropriate amount of dilute ammonia solution was added to adjust pH value of the solutions to 4. The solutions were then transferred into different quartz crucibles and heated on a hot plate. With the evaporation of water, the solutions gradually became from sol to gel. Finally, combustion reaction took place within a few minutes, and white fluffy powders were formed. The as-synthesized powders were calcined at 800°C for 2 h and then ball-milled for 20 h. The milled powders were dried, sieved and bidirectionally pressed into pellets ($\varnothing 20 \times 2.5$ mm) at 20 MPa, which were further cold isostatically pressed at 200 MPa. The pellets were pre-sintered at 1000°C for 3 h in air, and then sintered at 1830°C for 6 h in vacuum. The obtained ceramics were annealed at 1500°C for 5 h in air and then polished on both sides to a thickness of 1 mm for test.

Phase compositions of the ceramics were analyzed by X-ray diffraction (XRD, Bruker, D8 Focus diffractometer, Germany) with $\text{Cu K}\alpha$ radiation ($\lambda = 0.15418$ nm) in the range of $2\theta = 10$ – 80° . In-line transmittance of the transparent ceramics was measured using a UV-VIS spectrophotometer (Purkinje General, TU-1810, China) in the range of 200–1100 nm. The photoluminescence (PL) excitation and emission spectra were measured by a spectrofluorometer (Horiba, Fluoromax-4, Japan).

3. Results and discussion

Fig. 1 shows the XRD patterns of Eu^{3+} -doped $\text{La}_{0.8}\text{Gd}_{1.2}\text{Hf}_2\text{O}_7$ transparent ceramics vacuum-sintered at 1830°C for 6 h and annealed at 1500°C for 5 h in air. Compared with the undoped ceramics, all the ceramics exhibit pyrochlore structure with the characteristic peaks of pyrochlore phase corresponding to (331) and (511) reflections [18]. Due to the fact that the ionic radius of Eu^{3+} ($r_{\text{Eu}}^{3+} = 1.066$ Å) is smaller than that of La^{3+} ($r_{\text{La}}^{3+} = 1.160$ Å), the diffraction peaks of the ceramics slightly shift to higher angle as Eu^{3+} doping content increases, which can be clearly seen from the enlarged diffraction peak corresponding to (622) reflection (Fig. 1,

the right part).

Fig. 2 shows a photo of the polished Eu^{3+} -doped $\text{La}_{0.8}\text{Gd}_{1.2}\text{Hf}_2\text{O}_7$ transparent ceramics before and after annealing at 1500°C for 5 h in air. All the ceramics exhibit high optical transparency. Before annealing, the ceramics presented orange red color, and the color became darker as Eu^{3+} doping content increased. The color derived from oxygen vacancy and other defects due to vacuum sintering, which can produce strong light absorption through the formation of color centers. With the increase of Eu^{3+} doping content, lattice distortion increased as well. Hence, the oxygen vacancy and other defects also increased, resulting in the darker color. While, after annealing in air, the oxygen vacancy and other defects in the ceramics were eliminated and the orange red color of the ceramics faded away.

The in-line transmittance curves of the unannealed and annealed Eu^{3+} -doped $\text{La}_{0.8}\text{Gd}_{1.2}\text{Hf}_2\text{O}_7$ transparent ceramics (1.0 mm thick) are shown in Fig. 3. The transmittance of the unannealed ceramics was lower than that of the annealed ceramics, especially in the short wavelength region, where the incident light was absorbed by color centers. As Eu^{3+} doping content increased, the Eu^{3+} absorption increased as well, which led to the decrease of transmittance for both the annealed and unannealed ceramics. For the ceramics unannealed, the cut-off edge of the transmittance curves occurred redshift with the increasing of Eu^{3+} doping content, indicating that the energy band of the unannealed ceramics became narrow because of the existence of impurity levels, which derived from oxygen vacancy and other defects. After annealing, the impurity levels were eliminated and the energy band of the ceramics became normal. Besides, the absorption peaks of Eu^{3+} can be seen on the transmittance curves for the annealed ceramics, and they became stronger as Eu^{3+} doping content increased.

The PL excitation and emission spectra of the ceramics are shown in Fig. 4 (unannealed) and Fig. 5 (annealed), respectively. The luminescence intensity of unannealed ceramics (slit width = 4 nm) was very weak compared with the annealed ceramics (slit width = 2 nm). Thus, the slit width of the spectrometer was set differently.

Fig. 4a shows the excitation spectra of the unannealed ceramics, and the detection wavelength was 585 nm. The strong broad band around 285 nm was attributed to the charge transfer (CT) band transition between metal cations and oxygen ions. As Eu^{3+} doping content increased, the luminescence intensity decreased. The CT band center slightly shifted from 287 nm (1 at% Eu^{3+}) to 281 nm (10 at% Eu^{3+}), indicating the CT energy became larger. This resulted from the shorter distance between cations and the surrounding oxygen ions ($r_{\text{Eu}}^{3+} < r_{\text{La}}^{3+}$). In contrast, the other luminescence peaks

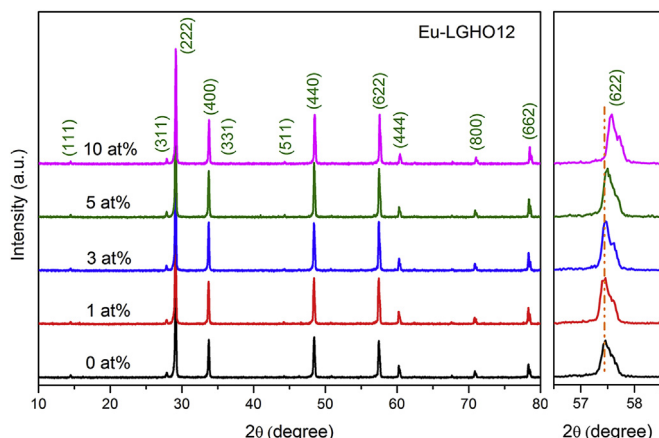


Fig. 1. XRD patterns of Eu^{3+} -doped $\text{La}_{0.8}\text{Gd}_{1.2}\text{Hf}_2\text{O}_7$ transparent ceramics.

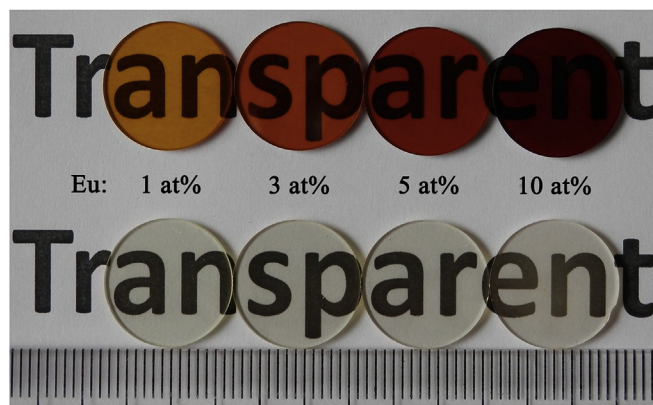


Fig. 2. Photograph of unannealed (above) and annealed (below) Eu^{3+} -doped $\text{La}_{0.8}\text{Gd}_{1.2}\text{Hf}_2\text{O}_7$ transparent ceramics.

Download English Version:

<https://daneshyari.com/en/article/5442533>

Download Persian Version:

<https://daneshyari.com/article/5442533>

[Daneshyari.com](https://daneshyari.com)